

# Modelling thermostating, entropy currents and cross effects by dynamical systems

Jürgen Vollmer<sup>(1,2)</sup>, Tamás Tél,<sup>(3)</sup> and László Mátyás<sup>(3)</sup>

*(1) Fachbereich Physik, Univ.-GH Essen, 45117 Essen, Germany.*

*(2) Max-Planck-Institut for Polymer Research, Ackermannweg 10, 55128 Mainz, Germany.*

*(3) Institute for Theoretical Physics, Eötvös University, P. O. Box 32, H-1518 Budapest, Hungary.*

(February 8, 2008)

A generalized multibaker map with periodic boundary conditions is shown to model boundary-driven transport, when the driving is applied by a “perturbation” of the dynamics localised in a macroscopically small region. In this case there are sustained density gradients in the steady state. A non-uniform stationary temperature profile can be maintained by incorporating a heat source into the dynamics, which deviates from the one of a bulk system only in a (macroscopically small) localized region such that a heat (or entropy) flux can enter an attached thermostat only in that region. For these settings the relation between the average phase-space contraction, the entropy flux to the thermostat and irreversible entropy production is clarified for stationary and non-stationary states. In addition, thermoelectric cross-effects are described by a multibaker chain consisting of two parts with different transport properties, modelling a junction between two metals.

## I. INTRODUCTION

There is a recent interest in modelling transport processes by simple dynamical systems with chaotic dynamics. One class of models, actually inspired by non-equilibrium molecular dynamics (NEMD) simulations, describes systems driven by external fields with a spatially uniform dynamics subjected to periodic boundary conditions [1–7]. Another approach concentrates on systems driven from the boundaries, which lead to steady states with sustained gradients of the thermodynamic fields [8,9]. For a comparatively simple, but as far as their transport properties are concerned, generic class of dynamical systems, the *multibakers*, [10–20] we show that both mechanisms of driving can simultaneously be worked out. This leads to an improved understanding of the relation between the approaches. In the former approach transport is driven by a field acting uniformly in the full system, while in the latter case the driving is concentrated to a microscopic region in space. From this point of view, boundary-driven transport is closely analogous to transport in a dynamical system with periodic boundary conditions, which is driven out of equilibrium by a “perturbation” of the dynamics, localised in a macroscopically small region.

In all models for transport, as emphasized by Nicolis and coworkers [24,25], a quantity of central interest is the heat flux, or equivalently the entropy flux, from the system into its environment. A central aim of modelling transport by dynamical systems is to identify settings, which are consistent with the thermodynamic entropy balance

$$\frac{dS}{dt} = \frac{d_e S}{dt} + \frac{d_i S}{dt}, \quad (1)$$

i.e., with the statement that the temporal change of the thermodynamic entropy  $S$  can be decomposed into two contributions, called the external and internal change of the entropy, respectively. This integral form can be rewritten into a local balance equation when the two terms on the right hand side correspond to integrals of local densities. In that case, the time derivative of the entropy density  $s$  appears as

$$\partial_t s = \Phi + \sigma^{(irr)} \quad (2)$$

where  $\Phi$  and  $\sigma^{(irr)}$  represent the densities of the entropy flux and the rate of irreversible entropy production, respectively. In the bulk of typical macroscopic systems the entropy flux can be written as the divergence of the entropy current  $j^{(s)}$ ,

$$\Phi = -\nabla j^{(s)}, \quad (3)$$

reflecting the fact that no heat can be taken out from the system locally [21]. On the other hand, this form has to be generalized at positions where there is a heat current flowing into an attached thermostat, and in cases where the entropy current is not differentiable, like for instance across interfaces between different materials. In those cases the entropy flux is not a full divergence, and it need not even be defined as a density. Rather the flux should then be written as

$$\Phi = -\nabla j^{(s)} + \Phi^{(th)}, \quad (4)$$

where  $j^{(s)}$  is still the entropy current flowing in the system, but  $\Phi^{(th)}$  accounts for the heat taken out in the form of a direct flow into the surroundings, which acts then as a thermostat.

In the present paper, we shall put special emphasis on the role of the entropy flux  $\Phi^{(th)}$ , and on exploring under which conditions it can vanish. We find conditions on how to model the entropy balance for thermodynamic bulk systems, and for macroscopic systems, which are subjected to thermostating by either a localized sink for the entropy or a spatially uniform coupling to a thermostat.

The role of the thermodynamic entropy of dynamical systems is played by the coarse-grained Gibbs entropy, whose usefulness in understanding irreversibility from the point of view of dynamical systems is by now thoroughly explained in the literature [22–27, 12–20]. (For stochastically perturbed dynamical systems where noise generates a kind of coarse graining, see [24, 25]). The bulk dynamics is represented by a multibaker model driving two fields, the density  $\varrho$  and the kinetic energy per particle  $T$ , with a local source density  $q$  for the latter [17, 18]. A connection with macroscopic transport equations is aimed at in a suitable defined continuum limit (the *macroscopic limit*), where the field  $T$  will be interpreted as a temperature, based on the experience that this quantity is closely related to the average kinetic energy per particle.

We shall consider a sequence of periodic models of increasing complexity. Model I corresponds to a homogeneous isothermal system described by a thermostating algorithm. In this model no entropy current is defined — its entire entropy flux stems from a  $\Phi^{(th)}$ . By allowing a spatial resolution of the isothermal system (Model II), a non-vanishing  $-\nabla j^{(s)}$  term appears in the transient behaviour, but  $\Phi^{(th)}$  remains unchanged. It is the only contribution to the flux in a steady state. Model III is still isothermal but with a locally deviating dynamics in one of the multibaker cells representing a boundary. The bulk dynamics can then be chosen so that (3) holds in the bulk, and all the heat taken out is concentrated in the boundary with a  $\Phi^{(th)} \neq 0$  there. In model IV we allow for temperature changes and local heat sources. By taking  $q$  locally deviating from that of the bulk in one cell, we find a steady temperature profile with a break at the boundary. The  $q$  distribution can then be chosen such that again (3) holds in the bulk. The heat source in the boundary is however singular. It corresponds exactly to the one which follows from thermodynamics. Finally, we consider a multibaker chain joined together from two subchains with different material properties. This models a junction between two metals so that one can observe thermodynamic cross effects, like the Peltier and Seebeck effects, very much in the same arrangements as in classical experiments.

This paper is organized as follows. In Section II the local dynamics of the considered multibaker model is defined, and its local entropy balance is worked out. In Section III, Model I – Model IV are treated, which share periodic boundary conditions and represent thermodynamic settings of increasing complexity. Section IV is devoted to cross-effects. We conclude with a short discussion in Section V.

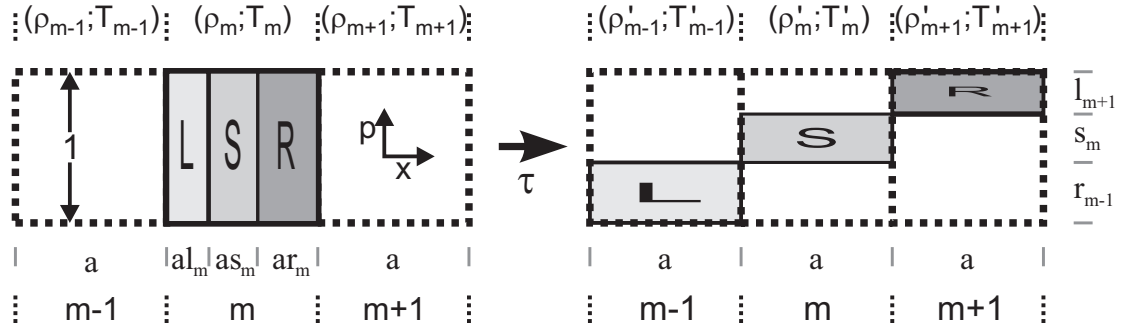


FIG. 1. Graphical illustration of the action of the multibaker map on cell  $m$ . The letters  $L$ ,  $S$  and  $R$  are inserted to visualize this action. Iteration of the rule after every time unit  $\tau$  defines the time evolution. More details about the action of the mapping and the symbols needed for its definitions are given in the text. The symbols  $\varrho_i$  and  $T_i$  indicated on the margins show the average values of the fields on the cells and on its neighbors  $i = m \pm 1$ .

## II. LOCAL TRANSPORT AND THERMODYNAMIC RELATIONS FOR MULTIBAKERS

In this section we describe the local dynamics of a cell of a multibaker map modelling a system with particle [20, 12, 14–16] and heat transport [17, 18]. We work out its density and kinetic-energy dynamics, and present general relations for the entropy changes. The effect of boundary conditions will be considered in subsequent sections for a few models with progressively richer thermodynamics.

The phase space  $(x, p)$  of the multibaker map consists of cells labelled by the index  $m$  (Fig. 1). The division of the  $x$  axis into cells corresponds to a partitioning of the configuration space into regions, sufficiently large to allow to characterize the state inside the cell by thermodynamic variables and small enough to neglect variation of these

variables on the length scale of the cells (*local equilibrium approximation*). Every cell has a width  $a$  and height  $b \equiv 1$ . The coordinates of individual particles in the cell are given as a position variable  $x$ , and a momentum-like variable  $p$ . We are interested in the dynamics of two dimensionless fields, the phase-space density  $\varrho(x, p)$ , and a field  $T(x, p)$  characterizing the local kinetic energy per particle. After each time unit  $\tau$ , every cell is divided into three columns (Fig. 1) with respective widths  $al_m$ ,  $as_m$  and  $ar_m$ . (Note that  $l_m + s_m + r_m = 1$  for any  $m$ .) The right (left) column of width  $ar_m$  ( $al_m$ ) is uniformly squeezed and stretched into a strip of width  $a$  and of height  $l_{m+1}$  ( $r_{m-1}$ ), which is mapped to the right (left) neighbouring cell. The middle one preserves its area and remains in cell  $m$ . Note that the map is one-to-one on its domain. It globally preserves the phase-space volume, but it can *nevertheless* locally expand or contract the phase-space volume. In Ref. [14,18] it was argued that only the choice of the contraction factors given here can be consistent with thermodynamics (in fact, one can find an analogous formulation with a fully area preserving dynamics at the expense of a spatial variation of the volume of the cells of the multibaker; cf. [19]).

The field  $T$  is advected by the particle dynamics, and — in order to mimic a local heating of the system — it is also multiplied by a factor  $(1 + \tau q)$  depending on the averages characterizing the local currents and the thermodynamic state. By this a *mean-field-like* coupling of the motion of the particles in and around of a given cell is introduced. In general, the width of the columns may depend on the variables characterizing the thermodynamic state in the vicinity of the cell, so that they vary in time and space. This is indicated by the explicit dependence of the parameters on the cell index. Iteration of these rules defines the time evolution of the system. The  $(x, p)$  dynamics generates ever refining structures in the distributions  $\varrho(x, p)$  and  $T(x, p)$ . For simplicity, we take the fields initially constant in each cell:  $\varrho(x, p) = \varrho_m$ ,  $T(x, p) = T_m$ .

### A. Dynamics of the particle density and the particle current

After one step of iteration, the fields will be piecewise constant on the strips defined in Fig. 1. Due to the conservation of particles, the phase-space density takes the respective values

$$\varrho'_{m,r} = \frac{r_{m-1}}{l_m} \varrho_{m-1}, \quad \varrho'_{m,s} = \varrho_m, \quad \varrho'_{m,l} = \frac{l_{m+1}}{r_m} \varrho_{m+1}. \quad (5)$$

(The prime will always indicate quantities evaluated after one time step.) The contraction factors  $r_{m-1}/l_m$  and  $l_{m+1}/r_m$  contribute to the (weighted) local phase-space contraction  $\sigma_m$  of cell  $m$ :

$$\sigma_m = \frac{1}{\tau} \left[ \varrho_{m-1} r_{m-1} \ln \frac{r_{m-1}}{l_m} + \varrho_{m+1} l_{m+1} \ln \frac{l_{m+1}}{r_m} \right]. \quad (6)$$

After one time step, the average density  $\varrho'_m$  in cell  $m$  is determined by its initial density  $\varrho_m$  and by the initial densities  $\varrho_{m\pm 1}$  of the neighbouring cells. Multiplying the strip densities (5) with the widths of the respective strips, adding them up and dividing the sum by the width  $a$  of the cell, one obtains the average (or the *coarse-grained*) density after the iteration

$$\varrho'_m = s_m \varrho_m + r_{m-1} \varrho_{m-1} + l_{m+1} \varrho_{m+1}. \quad (7)$$

The coarse-grained density evolves according to this master equation, which can be rearranged to obtain the discrete conservation law of the density

$$\frac{\varrho'_m - \varrho_m}{\tau} = - \frac{j_m - j_{m-1}}{a}. \quad (8)$$

Here

$$j_m = \frac{a}{\tau} (r_m \varrho_m - l_{m+1} \varrho_{m+1}) \quad (9)$$

is the discrete particle current flowing through the right boundary of cell  $m$ .

### B. The kinetic-energy dynamics and the energy current

According to the  $T$  dynamics described above, the updated values  $T'_{m,r}$ ,  $T'_{m,s}$ ,  $T'_{m,l}$  for  $T$  on the respective strips  $R$ ,  $S$ ,  $L$  of cell  $m$  contain a source term characterized by a local strength  $q_m$ :

$$\begin{aligned}
T'_{m,r} &= T_{m-1} [1 + \tau q_m], \\
T'_{m,s} &= T_m [1 + \tau q_m], \\
T'_{m,l} &= T_{m+1} [1 + \tau q_m].
\end{aligned} \tag{10}$$

This strength is yet undetermined. It depends on the physical setting of thermostating to be modelled and on the average of  $\varrho$  and  $T$  values in the cells and in its neighbours.

The  $(x, p)$  dynamics also drives the field  $T$ , i.e., after one iteration the kinetic-energy density of cell  $m$  takes the value

$$\varrho'_m T'_m = [s_m \varrho_m T_m + r_{m-1} \varrho_{m-1} T_{m-1} + l_{m+1} \varrho_{m+1} T_{m+1}] (1 + \tau q_m). \tag{11}$$

This equation can be rearranged as a discrete balance equation for the time evolution of  $\varrho T$ :

$$\frac{\varrho'_m T'_m - \varrho_m T_m}{\tau} = \varrho'_m T'_m \frac{q_m}{1 + \tau q_m} - \frac{j_m^{(\varrho T)} - j_{m-1}^{(\varrho T)}}{a}, \tag{12}$$

where  $j_m^{(\varrho T)} = T_m j_m - (a^2 l_{m+1}/\tau) \varrho_{m+1} (T_{m+1} - T_m)/a$  is a corresponding discrete energy current. Note that the r.h.s of (12) is not a full divergence, in accordance with the fact that the kinetic energy is not a conserved quantity. In an isothermal system where there is no kinetic energy dynamics, no source can be present ( $q_m = 0$ ).

### C. Gibbs entropy and the coarse-grained entropy

In this study we are interested in both the temporal evolution of the exact fields  $\varrho(x, p)$  and  $T(x, p)$ , and in the evolution of their respective cell averages  $\varrho_m$  and  $T_m$ . The former densities characterize the microscopic time evolution, while the averages describe the local thermodynamic state in spatially small regions. Both levels of description admit entropy functionals, which are commonly denoted as Gibbs and coarse-grained entropy.

The Gibbs entropy  $S^{(G)}$  is related to the detailed knowledge of the system. It is taken with respect to the exact densities  $\varrho(x, p)$  and  $T(x, p)$ . In a given cell it is defined as

$$S_m^{(G)} = - \int_{\text{over cell } m} dx dp \varrho(x, p) \ln \left( \frac{\varrho(x, p)}{\varrho^*} T(x, p)^{-\gamma} \right). \tag{13}$$

Here  $\varrho^* T^\gamma$  plays the role of a local  $T$ -dependent reference density with a constant reference density  $\varrho^*$  and  $\gamma$  an as yet undetermined constant.

The coarse-grained entropy  $S_m$  has a similar form, but it is based on the averaged values in the considered cell:

$$S_m = -a \varrho_m \ln \left( \frac{\varrho_m}{\varrho^*} T_m^{-\gamma} \right). \tag{14}$$

As mentioned above, throughout the paper we only consider initial distributions, which are uniform in every cell (cf. [14,16,18] for more general choices). As a consequence, initially  $S_m = S_m^{(G)}$ , and after one time step the entropies become

$$S_m^{(G)'} = -a \left[ s_m \varrho_m \ln \left( \frac{\varrho_m}{\varrho^*} T_{m,s}'^{-\gamma} \right) + r_{m-1} \varrho_{m-1} \ln \left( \frac{\varrho'_{m,r}}{\varrho^*} T_{m,r}'^{-\gamma} \right) + l_{m+1} \varrho_{m+1} \ln \left( \frac{\varrho'_{m,l}}{\varrho^*} T_{m,l}'^{-\gamma} \right) \right], \tag{15}$$

and

$$S'_m = -a \varrho'_m \ln \left( \frac{\varrho'_m}{\varrho^*} T_m'^{-\gamma} \right). \tag{16}$$

### D. Entropy balance

The coarse-grained entropy fulfills a local entropy balance in direct analogy to the one in irreversible thermodynamics. To derive this equation one identifies at any given time the difference  $S_m - S_m^{(G)}$  as the information on the microscopic state of the system, which cannot be resolved in the coarse-grained description. The temporal change of this lack of information is then identified with the irreversible entropy production  $\Delta_i S_m$ , and the change  $(S_m^{(G)} - S_m^{(G)})$  of the Gibbs entropy with the entropy flux  $\Delta_e S_m$ . Thus,

$$\frac{S'_m - S_m}{\tau} = \frac{\Delta_e S_m}{\tau} + \frac{\Delta_i S_m}{\tau} \quad (17)$$

which is a discrete analog of (1).

The form of the entropy production is [cf. (15) and (16)]:

$$\begin{aligned} \frac{\Delta_i S_m}{\tau} &= \frac{[S'_m - S_m^{(G)'}] - [S_m - S_m^{(G)}]}{\tau} \\ &= \frac{a}{\tau} \left[ -\varrho'_m \ln \left( \frac{\varrho'_m T_m'^{-\gamma}}{\varrho_m T_m'^{-\gamma}} \right) + \varrho_{m-1} r_{m-1} \ln \left( \frac{\varrho'_{m,r} T_{m,r}'^{-\gamma}}{\varrho_m T_{m,s}'^{-\gamma}} \right) + \varrho_{m+1} l_{m+1} \ln \left( \frac{\varrho'_{m,l} T_{m,l}'^{-\gamma}}{\varrho_m T_{m,s}'^{-\gamma}} \right) \right], \end{aligned} \quad (18)$$

where we used that  $S_m - S_m^{(G)}$  vanishes due to the particular choice of initial conditions.

The entropy flux becomes

$$\frac{\Delta_e S_m}{\tau} = -\frac{a}{\tau} \left[ (\varrho'_m - \varrho_m) \ln \left( \frac{\varrho_m T_m'^{-\gamma}}{\varrho^* T_m'^{-\gamma}} \right) + \varrho'_m \ln \frac{T_{m,s}'^{-\gamma}}{T_m'^{-\gamma}} + \varrho_{m-1} r_{m-1} \ln \left( \frac{\varrho'_{m,r} T_{m,r}'^{-\gamma}}{\varrho_m T_{m,s}'^{-\gamma}} \right) + \varrho_{m+1} l_{m+1} \ln \left( \frac{\varrho'_{m,l} T_{m,l}'^{-\gamma}}{\varrho_m T_{m,s}'^{-\gamma}} \right) \right] \quad (19)$$

which can be split into a divergence of an entropy current and a flux into the thermostat

$$\frac{\Delta_e S_m}{a\tau} = -\frac{j_m^{(s)} - j_{m-1}^{(s)}}{a} + \Phi_m^{(th)} \quad (20)$$

with

$$j_m^{(s)} \equiv -j_m \ln \left( \frac{\varrho_m T_m'^{-\gamma}}{\varrho^* T_m'^{-\gamma}} \right) + \frac{a l_{m+1}}{\tau} \varrho_{m+1} \ln \left( \frac{\varrho_{m+1} T_{m+1}'^{-\gamma}}{\varrho_m T_m'^{-\gamma}} \right) - \varrho_m v_m, \quad (21a)$$

$$\begin{aligned} \Phi_m^{(th)} &\equiv -\frac{1}{\tau} \left[ \varrho'_m \ln \frac{T_{m,s}'^{-\gamma}}{T_m'^{-\gamma}} + r_{m-1} \varrho_{m-1} \ln \left( \frac{r_{m-1} T_{m,r}'^{-\gamma} T_m'^{-\gamma}}{l_m T_{m,s}'^{-\gamma} T_{m-1}'^{-\gamma}} \right) + l_{m+1} \varrho_{m+1} \ln \left( \frac{l_{m+1} T_{m,l}'^{-\gamma} T_m'^{-\gamma}}{r_m T_{m,s}'^{-\gamma} T_{m+1}'^{-\gamma}} \right) \right] \\ &\quad - \frac{v_m \varrho_m - v_{m-1} \varrho_{m-1}}{a}. \end{aligned} \quad (21b)$$

Note that (20) is a discrete counterpart of (4), and  $j_m^{(s)}$  and  $\Phi_m^{(th)}$  are the discrete entropy current and entropy flux to the thermostat, respectively.

### E. The macroscopic limit

The projection of the multibaker dynamics on the  $x$  axis corresponds to a biased random walk with some diffusion coefficient and drift. The drift has to be present if we want to model nonequilibrium systems subjected to electric fields and/or temperature gradients. The requirement of consistency with an advection diffusion equation in the large system and long time limit, when the cell size is much smaller than the system size, and the time unit is much shorter than the macroscopic relaxation time, leads [12,14,15,17] to the scaling relation:

$$r_m = \frac{\tau D}{a^2} \left( 1 + \frac{a v_m}{2D} \right), \quad (22a)$$

$$l_m = \frac{\tau D}{a^2} \left( 1 - \frac{a v_m}{2D} \right). \quad (22b)$$

Here we allow for a location dependence of the drift  $v_m$  but assume the diffusion coefficient  $D$  to be spatially constant. The continuum limit of the multibaker dynamics, which is taken with these constraints, is called the *macroscopic limit*. Formally, it corresponds to taking  $a, \tau \rightarrow 0$  while keeping  $D$  fixed, and  $am, \varrho_m, T_m, v_m$  and  $q_m$  finite so that they approach a macroscopic position coordinate  $x$ , and smooth functions  $\varrho(x)$ ,  $T(x)$ ,  $v(x)$  and  $q(x)$ , respectively. After taking this limit we call  $\varrho(x)$  the density and  $T(x)$  temperature distribution in the system. The macroscopic limit of all the local relations given in (7)–(19) can be worked out explicitly [12,14,15,17]. In the following this limit will be indicated by an arrow ‘ $\rightarrow$ ’. Here we only mention that the system’s equation of state turns out [17,18] to be that of classical ideal gas with  $\gamma\varrho$  as its heat capacity (measured in units of Boltzmann’s constant).

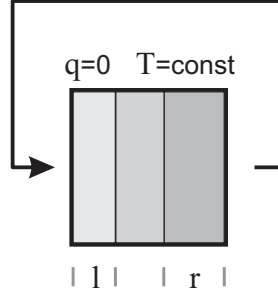


FIG. 2. Isothermal single-cell periodic baker map. The right boundary is identified with the left one.

### III. PERIODIC MODELS

#### A. Model I: Isothermal single-cell multibaker

We start by discussing the simplest conceivable model for describing a macroscopic transport process. A particle current induced by an external field in an isothermal environment described by a single baker cell subjected to periodic boundary conditions. The right boundary of the cell is identified with its left boundary and the mapping is from the cell onto itself. Because of driving  $r \neq l$ , and thermostating is applied via the appearance of the contraction rates  $l/r$  and  $r/l$  in order to reach a steady state. This mapping propagates the coordinates of a large number of particles, which do not interact, i.e., they all are mapped by the same mapping. Clearly, this system does not admit a spatial resolution of the densities characterizing the transport process. Its local and global behaviour coincides, so that the subscript  $m$  of the densities can be discarded in this case.

For the single-cell multibaker the master equation (7) predicts  $\varrho' = \varrho \equiv \bar{\varrho}$ . This implies that the model describes transport in a steady state with the average density  $\bar{\varrho}$ . The particle current  $j = (a/\tau)(r-l)\bar{\varrho} = v\bar{\varrho}$  is constant in space and time, and the entropy production (18) becomes ( $T = \text{const.}$ ).

$$\frac{\Delta_i S}{a\tau} = \bar{\varrho} \frac{(r-l)}{\tau} \ln \left( \frac{r}{l} \right) \equiv \sigma \quad (23)$$

which has the macroscopic limit:

$$\frac{\Delta_i S}{a\tau} \rightarrow \sigma^{(irr)} = \bar{\varrho} \frac{v^2}{D}. \quad (24)$$

In a similar way, the entropy flux (20, 21b) has the macroscopic form:

$$\frac{\Delta_e S}{a\tau} \rightarrow \Phi^{(th)} = -\bar{\varrho} \frac{v^2}{D} \quad (25)$$

As expected in a steady state,  $\Delta_i S$  and  $\Delta_e S$  add up to zero. More interestingly, however, these contributions to the change of entropy are also directly proportional to the local phase-space contraction (6), which reduces to  $\bar{\varrho} v^2/D$  in the macroscopic limit.





whose increment  $\delta\varrho$  is uniquely determined by  $r_0$  (or  $v_0$ ). In cell zero we find  $\varrho_0 = \bar{\varrho}$ . A substitution into the master equation for  $m = 1$  or  $N$  leads to

$$\delta\varrho = \bar{\varrho} \frac{2}{N+1} \left( \frac{r_0}{r} - 1 \right). \quad (37)$$

Again the average density  $\bar{\varrho}$  is related to the number of particles  $\mathcal{N}$  in the system via  $a\bar{\varrho}(N+1) = \mathcal{N}$ . By taking into account that according to (22)  $r_0 = r[1 + av_0/(2D)]$ , we obtain that  $\delta\varrho$  is indeed proportional to  $v_0$ :

$$v_0 = D \frac{\delta\varrho}{a} \frac{N+1}{\bar{\varrho}} = D \frac{\delta\varrho}{a} \frac{\mathcal{N}}{a\bar{\varrho}^2}. \quad (38)$$

The steady state current is:

$$j = \bar{\varrho} \frac{v_0}{2} - D \frac{\varrho_1 - \bar{\varrho}}{a} = D \frac{\delta\varrho}{a} = \frac{v_0 \bar{\varrho}}{N+1}. \quad (39)$$

The diffusion current of cells  $N$  and  $0$  is much stronger than otherwise, due to the sudden jump in the densities, but in the steady state the surplus is exactly compensated by the local drift currents. Thus the particle transport in the steady states of Model II and Model III are equivalent provided the drift  $v$  in the former coincides with  $D\delta\varrho/(a\bar{\varrho})$  in the latter. As far as the steady state transport is concerned, it does not matter, whether one applies a small uniform field leading to a spatially uniform drift  $v$  or a large one  $v_0 = (N+1)v$  in a single cell only.

All thermodynamic relations of relevance can be worked out not only for the steady state (36), but for general non-steady states. The local forms of the entropy production and the entropy flux in the bulk are special cases of (29)-(31). Since  $r = l$  in the bulk, there is no entropy flux flowing into the thermostat  $\Phi^{(th)} = 0$  for  $m = 2, \dots, N-1$ . On the other hand, the entropy flux in cell  $0$  and its neighbours does contain a part which cannot be written as a divergence. Due to (21b), the average density of the flux flowing into the thermostat turns out to be:

$$\begin{aligned} \Phi^{(th)} &\equiv \Phi_N^{(th)} + \Phi_0^{(th)} + \Phi_1^{(th)} = \frac{1}{\tau} \left[ (r\varrho_1 - r_0\varrho_0) \ln \left( \frac{r_0}{r} \right) - (r\varrho_N - l_0\varrho_0) \ln \left( \frac{r}{l_0} \right) \right] \\ &\approx \frac{v_0}{2} \frac{\varrho_1 - \varrho_N}{a} - \varrho_0 \frac{v_0^2}{4D} - \frac{\varrho_1 + \varrho_N}{2} \frac{v_0^2}{4D}. \end{aligned} \quad (40)$$

In the last approximation we have assumed that  $av_0 \ll 2D$ .

In the steady state  $\varrho_N - \varrho_1 = -(N-1)\delta\varrho = -(N-1)aj/D$ ,  $\varrho_0 = \frac{(\varrho_1 + \varrho_N)}{2} = \bar{\varrho}$ , and thus

$$\Phi^{(th)} \equiv -\frac{v_0 j}{D}. \quad (41)$$

In the macroscopic limit the quantity  $\delta\varrho/a$  approaches the gradient  $-\partial_x\varrho$  in the bulk,  $\bar{\varrho}$  and  $\mathcal{N}$  stay constant and thus  $v_0$  in (38) is proportional to  $1/a$ . The driving is singularly strong and so is the entropy flux density into the thermostat. By integrating, however, over the volume of cell zero and its neighbours we obtain the total entropy flux into the thermostat  $-av_0 j/D = -j^2 \mathcal{N}/\bar{\varrho}^2 D$ . It coincides with the macroscopic limit of the total entropy flux  $\sum_{m=0}^N \Delta_e S_m/\tau$  since the integral of  $\partial_x j^{(s)}$  vanishes in a periodic system, i.e.,

$$\frac{d_e S}{dt} = -\frac{j^2}{\bar{\varrho} D} \frac{\mathcal{N}}{\bar{\varrho}} \quad (42)$$

This result is equivalent to the steady state version of (35) expressed by the current.

In this model there is no need for taking out heat along the bulk, thermostating is active in cell  $0$  and its neighbours only. It extracts exactly the same entropy flux there as the full entropy flux of Model II in the steady state [8]. Thus the models refer to two different realizations of thermostating the transport process. Model II should be viewed as e.g. a wire which is kept at constant temperature by removing the heat due to dissipation everywhere along its length — Model III is closer related to a thermally isolated system, where heat is transported to the “boundary”, from where the system is driven. For the multibaker this takes place in the special cell  $m = 0$ . Boundary driven transport typically leads, however, to non-uniform temperature profiles. A full treatment of such transport processes should be based therefore on a multibaker chain with kinetic energy dynamics.

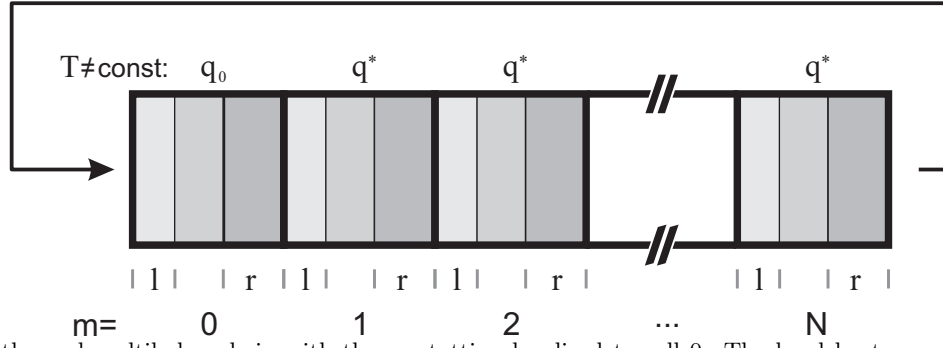


FIG. 5. Non-isothermal multibaker chain with thermostating localized to cell 0. The local heat source  $q_0$  of that cell is different from that in the bulk, which is  $q^* = -vj/D$ .

#### D. Model IV: Multibaker chain with thermostating localized to a single cell

In the realm of classical thermodynamics heat is transported to the boundaries of the system. If, however, there is a break in the temperature profile, a jump in the heat current occurs and heat is taken out at this point.

In order to model such a situation, we consider a multibaker chain with kinetic-energy dynamics. The general relation (18) and a calculation similar to the one leading to (29) yields in the macroscopic limit for the entropy production [18]

$$\sigma^{(irr)} = \lambda \left( \frac{\partial_x T}{T} \right)^2 + \frac{j^2}{\varrho D} \quad (43)$$

where  $j = \varrho v - D \partial_x \varrho$  is the particle current, and  $\lambda = \gamma \varrho D$  is the heat conductivity of the model. From (19)-(21b) we obtain

$$\Phi^{(th)} = \gamma \varrho q - \frac{vj}{D} \quad (44)$$

as the entropy flux let directly into the thermostat, and

$$j^{(s)} = -\lambda \frac{\partial_x T}{T} + \frac{e\Pi}{T} j, \quad (45)$$

as the entropy current with  $\Pi$  the bulk Peltier coefficient

$$\frac{e\Pi}{T} = - \left( 1 + \ln \frac{\varrho T^{-\gamma}}{q^*} \right). \quad (46)$$

Note that there is always a possibility to 'close' the system locally in the sense that the source term  $q = q^* = vj/\lambda$  is chosen such that  $\Phi^{(th)}$  vanishes.

We consider a periodic chain with fixed transition probabilities ( $r_m = r$ ,  $l_m = l$ ,  $m = 0, 1, \dots, N$ ). The local heating sources are assumed to be constant in the bulk:  $q_m = q^*$  for  $m = 1, \dots, N$  which differs from the source  $q_0$  of cell 0. In the steady state we find then a constant particle density along the chain. Inside the bulk, the kinetic-energy equation (11) implies for the steady temperature distribution

$$T_m = [(1 - r - l)T_m + rT_{m-1} + lT_{m+1}](1 + \tau q^*). \quad (47)$$

With periodic boundary conditions ( $T_{m=0} = T_0$ , and  $T_{m=N+1} = T_0$ ) this equation has the following general solution:

$$T_m = \frac{T_0}{\sin[b(N+1)]} \left( \frac{r}{l} \right)^{\frac{m}{2}} \left\{ \sin[b(N+1) - bm] + \left( \frac{l}{r} \right)^{\frac{N+1}{2}} \sin(bm) \right\} \quad (48)$$

where

$$\cos b = \sqrt{rl} \left( 1 - \frac{\tau q^*}{(1 + \tau q^*)(r + l)} \right). \quad (49)$$

The solution (48) has a break in cell zero, in the sense that the left and right derivatives are different. Only at the end of the system is the entropy flux not a full divergence. Applying the kinetic-energy equation (11) to cell zero in a steady state, where the density is constant, we find that:

$$q_0 = \frac{1}{\tau} \frac{r(T_0 - T_N) + l(T_0 - T_1)}{(1 - r - l)T_0 + rT_N + lT_1}. \quad (50)$$

In the macroscopic limit

$$aq_0 \rightarrow \frac{D}{T} \left[ \partial_x T|_{(-0)} - \partial_x T|_{(+0)} \right]. \quad (51)$$

This implies that the source density  $q_0$  is singular but the total source  $Q_0 = aq_0$  inside cell 0, is finite.

It is worth comparing this with the thermodynamic treatment of the same problem. If there is a jump in the entropy current, in order to have finite entropy flux density  $\Phi$  in each point, it is unavoidable to allow for a  $\tilde{\Phi}$  which is not a full divergence:

$$\Phi = -\partial_x j^{(s)} + \tilde{\Phi}. \quad (52)$$

The form of  $\tilde{\Phi}$  one obtains by integrating (52) around the point where the jump in the derivative appears ( $x = 0$ ):

$$\int_{-\epsilon}^{\epsilon} \Phi dx = -j^{(s)} \Big|_{(-\epsilon)}^{(+\epsilon)} + \int_{-\epsilon}^{\epsilon} \tilde{\Phi} dx. \quad (53)$$

The smoothness of  $\Phi$  implies that for  $\epsilon \rightarrow 0$

$$\int_{-\epsilon}^{\epsilon} \tilde{\Phi} dx = -j^{(s)} \Big|_{(-0)}^{(+0)}. \quad (54)$$

The multibaker result (44) implies that if  $q$  is singular as in cell 0, then  $\Phi_0^{(th)} = \gamma \varrho q_0$ . We then immediately see that  $\Phi_0^{(th)}$  is the analog of  $\tilde{\Phi}$ . Indeed, by inserting the expression (45) for  $j^{(s)}$  we have:

$$\int_{-\epsilon}^{\epsilon} \tilde{\Phi} dx = \frac{\lambda}{T} [\partial_x T|_{(+0)} - \partial_x T|_{(-0)}] \quad (55)$$

which, on account of  $\lambda = \gamma \varrho D$ , exactly corresponds to (50).

We have shown, that the thermodynamic evaluation and the macroscopic limit of  $q_0$  lead to the same result. Physically this means, that by a proper choice of the source terms even the singularity in the entropy flux can be described in full harmony with thermodynamics, and the flux let to flow in the thermostat is exactly the amount of heat what is taken out also in the thermodynamic description if a break appears.

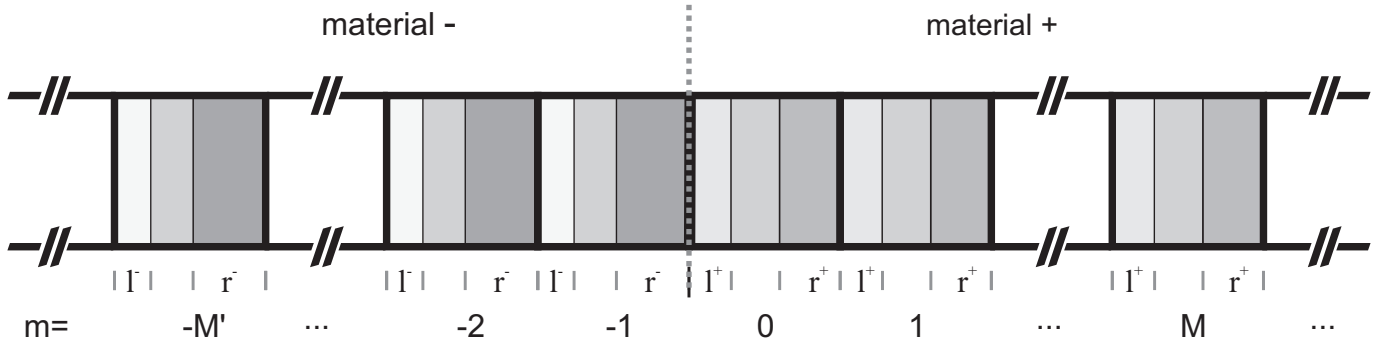


FIG. 6. Two long multibaker chains, representing materials - and +, joined together at the junction between cells -1 and 0. The leads are in cells  $-M'$  and  $M$ .

#### IV. CROSS EFFECTS IN A MULTIBAKER MODEL

Thermodynamic cross effects, which probe the (off-diagonal) Onsager coefficients, are difficult to observe in homogeneous systems. When two materials are put into contact, however, they play a dominant role in understanding

the heat and entropy currents. In order to mimick such phenomena, we consider two multibaker chains containing the cells  $m = -M' \cdots -1$  and  $m = 0 \cdots M$ , respectively,  $M, M' \gg 1$  which are brought into contact at  $m = 0$  (cf. Fig. 6). Now, the parameters  $l^-, s^-, r^-$  and  $l^+, s^+, r^+$  in the two parts are different, and for generality we will also assume that the constant reference densities  $\varrho^{\star, \pm}$  are different. These differences will represent the different thermodynamic and transport properties of the materials. The difference in  $r$  and  $l$  gives rise to different drifts (conductivities) and diffusion coefficients, and the one in the reference density might be thought of reflecting for instance a different effective mass of the electrons.

As in the previous subsection, the dynamics of this multibaker chain drives a density and a kinetic-energy field. In order to simplify the structure of the steady state density profiles, we restrict to the case  $r^+/l^+ = r^-/l^-$ . This choice is motivated by a physical interpretation of  $r/l$ . After all, the macroscopic limit of  $r/l$  is  $1 + av/D$ , and  $v/D$  is proportional to the external (electric) field, such that the requirement expresses that the external field should be the same in both materials. In the remainder of this section we discuss the transport in this model in two different settings: (i) a constant (non-vanishing) particle current and constant temperature; (ii) vanishing particle current and an isolated system which is only thermostatted at the “junction”  $m = 0$  and at the two “leads”  $m = -M'$  and  $m = M$ , respectively. Setting (i) allows us to discuss the Peltier effect and setting (ii) is used for the Seebeck effect.

Before turning to these specific settings, however, we discuss the steady state profile of the (particle) density in general. One does not expect noticable gradients in the electron density in either material, so that we fix them to the constant values  $\varrho^-$  and  $\varrho^+$ , leading to the spatially uniform current (cf. (9))

$$j = \frac{a}{\tau}(r^+ - l^+) \varrho^+ = \frac{a}{\tau}(r^- - l^-) \varrho^-.$$

In order to have the same current also across the junction, one has to require  $l^- \varrho^- = l^+ \varrho^+$  in addition. Together with the fact that  $v/D$  is fixed for the whole system, this implies that there is a constant amount of Joule’s heating  $vj/D$  per unit length of the system, which either has to be transferred to a local thermostat (cf. (44)), or leads to a local heating, i.e., enforces non-uniform temperature profiles.

### A. The Peltier effect

The requirement of a constant temperature in the setting of the Peltier effect requires the use of a thermostatted dynamics,  $q = 0$ . In that case the Joule heating is transferred to the thermostat. Away from the junction, this leads to the flux  $\Phi^{(th)} = vj/D$ . In the entropy balance the difference in the materials shows up *only* in the entropy currents. In view of (45), they become different in the two parts of the multibaker

$$j^{(s, \pm)} = -j \left( 1 + \ln \left[ \frac{\varrho^\pm}{\varrho^{\star \pm}} T^{-\gamma} \right] \right) = \frac{e \Pi^\pm}{T} j$$

implying that at the junction (i.e., between cells  $m = -1$  and  $m = 0$ ) an additional heat flux, the *Peltier heat*, is directed to the thermostat. It is characterized by the difference of the entropy currents

$$j^{(s, +)} - j^{(s, -)} = -j \ln \frac{\varrho^+/\varrho^{\star +}}{\varrho^-/\varrho^{\star -}} = j \left[ \ln \frac{l^+}{l^-} + \ln \frac{\varrho^{\star +}}{\varrho^{\star -}} \right] \equiv \frac{e \Pi^{(+/-)}}{T} j,$$

where  $\Pi^{(+/-)}$  defines the mutual Peltier coefficient of the two materials. It characterizes the amount of Peltier heat produced per unit electric current, and is the difference of the material Peltier coefficients [cf. (46)]

$$\Pi^{(+/-)} = \Pi^+ - \Pi^-. \quad (56)$$

as also found in thermodynamics.

### B. The Seebeck effect

The Seebeck effect is observed in a thermally isolated system, where the junction is kept at a temperature  $T_j$  different from the temperature  $T_l$  prescribed at the leads, i.e., for the multibaker we demand  $T_{-M'} = T_M = T_l$  and  $T_{-1} = T_0 = T_j$ . This setup corresponds to a non-uniform temperature field, and, due to this, also to gradients in the electro-chemical potential  $\mu$ . Because of the difference in the material properties, these gradients can add up to

a net potential drop between the leads, even if both leads are kept at the same temperature and there is no particle current. This follows immediately from the formal definition [21] of the particle current in its discrete version:

$$j_m = -\frac{\sigma_{el}}{e^2} \left[ \frac{\mu_{m+1} - \mu_m}{a} + e\alpha \frac{(T_{m+1} - T_m)}{a} \right], \quad (57)$$

where  $\sigma_{el}$  is the conductivity,  $e$  the electric charge, and  $\alpha$  the Seebeck coefficient of the material. In the considered system, we then have for vanishing current

$$\begin{aligned} \mu_{-M'} - \mu_M &= \mu_{-M'} - \mu_{-1} + \mu_{-1} - \mu_0 + \mu_0 - \mu_M \\ &\approx -e\alpha^- (T_{-M'} - T_{-1}) + \mu_{-1} - \mu_0 - e\alpha^+ (T_0 - T_M) = e(\alpha^+ - \alpha^-) (T_l - T_j) + \mu_{-1} - \mu_0. \end{aligned} \quad (58)$$

Here we have assumed the Seebeck coefficients to be approximately constant in the two materials. The macroscopic limit implies  $\mu_{-1} = \mu_0$ , and we obtain for the mutual Seebeck coefficient of the two materials [28]

$$\alpha^{(+/-)} \equiv \frac{\mu_{-M'} - \mu_M}{e(T_l - T_j)} = \alpha^+ - \alpha^-. \quad (59)$$

It characterizes the strength of the potential drop  $\mu_{-M'} - \mu_M$  between the leads induced by the temperature difference  $T_l - T_j$  between the leads and the junction.

An expression for  $\alpha^{(+/-)}$  can be determined for the multibaker by rewriting the expression (27) for the current in the form (57). Taking immediately the macroscopic limit and observing that the electro-chemical potential can be split into a chemical part  $\mu_c$  and a part  $e\phi$  due to the external electric field  $E \equiv -\partial_x \phi$ , one obtains

$$j = -\frac{\sigma_{el}}{e^2} [\partial_x(\mu_c + e\phi) + e\alpha \partial_x T] = \frac{\sigma_{el} E}{e} - \frac{\sigma_{el}}{e^2} [\partial_\varrho \mu_c \partial_x \varrho + \partial_T \mu_c \partial_x T + e\alpha \partial_x T] = v\varrho - D \partial_x \varrho. \quad (60)$$

Here

$$v = \frac{\sigma_{el} E}{e \varrho}, \quad (61a)$$

$$D = \frac{\sigma_{el}}{e^2} \partial_\varrho \mu_c, \quad (61b)$$

$$e\alpha = -\partial_T \mu_c. \quad (61c)$$

By the first two equations we recover well-known relations from thermodynamics [21]. Eq. (61c) provides us with a relation for the Seebeck coefficient. Since the equation of state of the “multibaker gas” is that of a classical ideal gas [18]

$$\mu_c^\pm = (\gamma + 1)T + T \ln \left( \frac{\varrho^\pm T^{-\gamma}}{\varrho^{*\pm}} \right),$$

one obtains

$$e\alpha^{(+/-)} = e(\alpha^+ - \alpha^-) = e \ln \frac{\varrho^+ T_l^{-\gamma}}{\varrho^{*+}} - e \ln \frac{\varrho^- T_l^{-\gamma}}{\varrho^{*-}} = e \left[ \ln \frac{l^+}{l^-} + \ln \frac{\varrho^{*+}}{\varrho^{*-}} \right] = \frac{e\Pi^{(+/-)}}{T_l},$$

where (56) was used in the last step. This comparison expresses the validity of the Onsager relation  $\Pi^{(+/-)} = \alpha^{(+/-)}T$  for this class of models.

## V. DISCUSSION

In this paper we have described the local and global transport properties of multibakers with a density and an energy dynamics. This class of maps makes an analytical modelling of transport processes by a deterministic chaotic dynamics possible, and admits a macroscopic description consistent with various aspects of irreversible thermodynamics. The macroscopic description comprises the time evolution of the average density and the kinetic energy in small regions of the physical space (the cells of the multibaker). The former density is interpreted as the particle density, and the latter as a temperature field. The averages in the small regions are in the spirit of local thermodynamic equilibrium, and the continuum description of thermodynamics arises in a macroscopic limit where the spatial resolution of the

transport process is small compared to the system size (or any other relevant macroscopic length), and where a discrete time-scale used in the definition of the dynamics is much smaller than macroscopic time scales.

The relevant concept of entropy for multibakers is the Gibbs entropy defined with respect to the average density in the cells normalized by a temperature-dependent reference density. It is called the coarse-grained entropy. Based on an information-theoretic interpretation of the entropy, a local entropy balance can be derived, which in the macroscopic limit can be fully consistent with irreversible thermodynamics. This agreement holds provided that (i) a particular choice of local phase-space contraction and expansion rates is incorporated in the time evolution of the density, which we identified as a time-reversible evolution of the mapping in previous work [12,14,15], (ii) the density in the entropy is normalized by a reference density with a power-law dependence on the average kinetic energy in the cell, and (iii) appropriate source terms are incorporated in the evolution equations of the kinetic-energy field. No meaningful macroscopic description can be found for multibakers with other choices of the phase-space contraction factors. Modification of the source terms leads to additional contributions in the local entropy balance, which are interpreted as local entropy fluxes into a thermostat. In particular, for vanishing source terms one can mimic a transport process in a system with a spatially uniform temperature, i.e., one obtains a setting reminiscent of NEMD simulations of transport processes.

Once the connection between the deterministic dynamics of the multibaker and the corresponding local thermodynamic relations is established, one can apply it to discuss transport in different macroscopic settings. A number of models with periodic boundary conditions were discussed in order to shed light on the global entropy balance in such systems. We find that, up to a trivial factor, the average phase-space contraction amounts to the entropy flux to the environment. This supports an earlier heuristic argument of Ruelle [22] and others [3–5], who connected the phase-space contraction to the irreversible entropy production in a steady state. In contrast to the claims of some of the latter authors (cf. for instance [29]) the connection between the irreversible entropy production and the phase-space contraction rate breaks down away from stationarity. In fact, the contraction rate is still connected to the entropy flux in that situation, but the flux is no longer related to the rate of irreversible entropy production. This was shown (a) for multibakers with a uniform thermostating (Model II), i.e., for models reminiscent of NEMD algorithms, (b) for systems where the driving and thermostating is applied in a macroscopically small region of the system (Model III), thus giving rise to sustained density gradients, and (c) systems with a uniform external field and localized thermostating (Model IV). The former two models have constant temperature fields, while the latter one supports a temperature profile with a discontinuity in the first derivative at the position of thermostating. As expected from the existence of the local entropy balance, the results are fully consistent with the corresponding thermodynamic description of the transport process. They suggest an interesting conclusion on modelling transport in bulk systems by isothermal NEMD simulations: These methods are valid in an approximation where the considered volume is sufficiently small to neglect density and temperature gradients. In steady states, they are equivalent to models, where the currents are the same, but thermostating is only applied at the boundaries of a macroscopic system. Since even state of the art simulations can hardly cope with more than  $10^9$  particles, i.e., with integration volumes larger than about  $\mu\text{m}^3$ , this approximation seems to be well-justified in numerical studies. On the other hand, this assumptions should be kept in mind when isothermal NEMD modelling is taken as basis of theoretical studies of transport processes (cf. for instance [3–5,27]).

To further demonstrate the use of multibakers with density and energy fields, we also discussed thermoelectric cross effects. The description of the transport properties requires in that case information on the equation of state, since the Seebeck effect is defined in terms of differences of chemical potentials. In previous work [17,18] it was shown that the classical ideal-gas equation holds for multibakers. This is meaningful since the time evolution of the multibaker can be considered as the one of particles with phase-space coordinates  $(x, p)$ , which only interact by a (weak) mean-field like coupling manifested in a dependence of the local parameters on the average densities. With this input the Peltier and Seebeck effect were modelled and the Onsager relation, connecting their respective transport coefficients, was derived. The validity of this relation for multibakers is not a trivial result. It heavily relies on the choices (i)–(iii) to find an entropy balance consistent with irreversible thermodynamics.

Summarizing, we demonstrated that multibakers establish a straightforward modelling of various transport phenomena by deterministic, chaotic dynamics. They give insight in the general structure of such models by explicit analytical calculations. This was demonstrated by discussions of thermoelectric cross effects, and of the relation between the average phase-space contraction, entropy fluxes and the rate of irreversible entropy production.

## ACKNOWLEDGMENTS

This work is dedicated to Prof. Gregoire Nicolis on occasion of his 60th birthday. Our discussions at the *Centre of Complex Systems and Nonlinear Phenomena* helped us a lot, when we were starting this project in the summer

of 1998. We are also grateful to J.R. Dorfman, B. Fogarassy, J. Hajdu, G. Tichy and H. Posch for enlightening discussions. The paper was completed during a joint stay at the *Max-Planck Institute for the Physics of Complex Systems*, which we gratefully acknowledge together with support from the Hungarian Science Foundation (OTKA T17493, T19483) and the TMR-network *Spatially extended dynamics*.

---

- [1] D.J. Evans and G.P. Morriss, *Statistical Mechanics of Nonequilibrium Liquids* (Academic Press, London, 1990); W.G. Hoover, *Computational Statistical Mechanics* (Elsevier, Amsterdam, 1991).
- [2] W.N. Vance, Phys. Rev. Lett. **69**, 1356 (1992).
- [3] N.I. Chernov, G.L. Eyink, J.L. Lebowitz, and Ya.G. Sinai, Phys. Rev. Lett. **70**, 2209 (1993); Comm. Math. Phys. **154**, 569 (1993).
- [4] D.J. Evans, E.G.D. Cohen, and G.P. Morriss, Phys. Rev. Lett. **71**, 2401 (1993).
- [5] G. Gallavotti and E.G.D. Cohen, Phys. Rev. Lett. **74**, 2694 (1995); J. Stat. Phys. **80**, 931 (1995).
- [6] K. Rateitschak, R. Klages and G. Nicolis, *Thermostatting by deterministic scattering: the periodic Lorentz gas*, chaos-dyn/9908013 (J. Stat. Phys., in press).
- [7] J.R. Dorfman, *An Introduction to Chaos in Non-Equilibrium Statistical Mechanics* (Cambridge Univ. Press, Cambridge, 1999); CHAOS **8**, No.2 (1998), Focus issue on *Chaos and Irreversibility*.
- [8] N.I. Chernov and J.L. Lebowitz, Phys. Rev. Lett. **75**, 2831 (1995); J. Stat. Phys. **86**, 953 (1997); Ch. Dellago and H.A. Posch, J. Stat. Phys. **88**, 825 (1997).
- [9] C. Wagner, R. Klages, and G. Nicolis, Phys. Rev. E **60**, 1401 (1999).
- [10] P. Gaspard, J. Stat. Phys. **68**, 673 (1992).
- [11] S. Tasaki and P. Gaspard, J. Stat. Phys. **81**, 935 (1995).
- [12] J. Vollmer, T. Tél, and W. Breymann, Phys. Rev. Lett. **79**, 2759 (1997).
- [13] P. Gaspard, Physica A **240**, 54 (1997); J. Stat. Phys. **88**, 1215 (1997).
- [14] J. Vollmer, T. Tél, and W. Breymann, Phys. Rev. E **58**, 1672 (1998).
- [15] W. Breymann, T. Tél, and J. Vollmer, CHAOS **8**, 396 (1998).
- [16] T. Gilbert, C.D. Ferguson, and J.R. Dorfman, Phys. Rev. E **59**, 364 (1999); T. Gilbert and J.R. Dorfman, J. Stat. Phys. **96**, 225 (1999).
- [17] L. Mátyás, T. Tél, J. Vollmer, *Cross-effects from dynamical systems*, chaos-dyn/9912028.
- [18] L. Mátyás, T. Tél, J. Vollmer, *A Multibaker Map for Cross-effects from dynamical systems*, chaos-dyn/9912034.
- [19] S. Tasaki and P. Gaspard, Theoretical Chemistry Accounts **102**, 385-396 (1999).
- [20] P. Gaspard, *Scattering, Chaos and Statistical Mechanics* (Cambridge Univ. Press, Cambridge, 1998).
- [21] S.R. de Groot and P. Mazur, *Nonequilibrium Thermodynamics* (Elsevier, Amsterdam, 1962) (reprinted: Dover, New-York, 1984).
- [22] D. Ruelle, J. Stat. Phys. **85**, 1 (1996); **86**, 935 (1997).
- [23] W. Breymann, T. Tél, and J. Vollmer, Phys. Rev. Lett. **77**, 2945 (1996).
- [24] G. Nicolis, D. Daems, J. Chem. Phys. **100**, 19187 (1996).
- [25] D. Daems, G. Nicolis, Phys. Rev. E **59**, 4000 (1999).
- [26] L. Rondoni and G.P. Morriss, Phys. Rev. E **53**, 2143 (1996).
- [27] G. Gallavotti, Phys. Rev. Lett. **77**, 4334 (1996); J. Stat. Phys. **86**, 907 (1997).
- [28] N. W. Ashcroft and N. D. Mermin, *Solid State Physics*, Chapter 16, (Holt, Reinehart and Winston, Saunders College, Philadelphia, 1976).
- [29] L. Rondoni and E.G.D. Cohen, *Gibbs entropy and Irreversible Thermodynamics* cond-mat/9908367.